Desalination and Water Treatment
www.deswater.com

doi: 10.1080/19443994.2014.951970

56 (2015) 1918–1928
November

Taylor & Francis
Taylor & Francis Group

Removal of malachite green (MG) from aqueous solutions by adsorption, precipitation, and alkaline fading using talc: kinetic, thermodynamic, and column feasibility studies

Young-Chul Lee[a,*], Minkee Choi[b], Ji-Won Yang[c], Hyun-Jae Shin[d,*]

[a]*Department of BioNano Technology, Gachon University, 1342 Seongnamdaero, Sujeong-gu, Seongnam-si, Gyeonggi-do 461-701, Republic of Korea, Tel. +82 31 750 8751; Fax: +82 42 865 8774; email: dreamdbs@gachon.ac.kr (Y.-C. Lee)*
[b]*Department of Chemical & Biomolecular Engineering (BK21 Program), KAIST, 335 Gwahak-ro, Yuseong-gu, Daejeon 305-701, Republic of Korea, Tel. +82 42 350 3938; Fax: +82 42 350 3924; email: mkchoi@kaist.ac.kr (M. Choi)*
[c]*Advanced Biomass R & D Center, KAIST, 291 Daehakno, Yuseong-gu, Daejeon 305-701, Republic of Korea, Tel. +82 42 350 3910; Fax: +82 42 350 3924; email: jwyang@kaist.ac.kr (J.-W. Yang)*
[d]*Department of Chemical & Biochemical Engineering, Chosun University, Seosuk-dong, Dong-gu, Gwangju 501-759, Republic of Korea, Tel. +82 62 230 7518; Fax: +82 62 230 7226; email: shinhj@chosun.ac.kr (H.-J. Shin)*

Received 1 March 2014; Accepted 30 July 2014

ABSTRACT

Malachite green (MG) has been widely used in the dyeing industry and as a fungicide and an antiseptic in the aquaculture industry. However, MG is very dangerous and cytotoxic to mammalian cells, and its discharge into receiving waters results in environmental problems in aquatic ecosystems. To remove this soluble dye from aqueous solutions, adsorption by inorganic clay is often used. In the case of the triphenylmethane dye family, molecular structure changes occur with changes in pH. As a result, chromatic MG^+ at a neutral pH turns into the protonated MG (MGH^{2+}) at an acidic pH and into the carbinol base form at a basic pH. In this study, taking into consideration the potential for MG structural change, batch sorption experiments for kinetics (5–1.17, 10–2.94, and 20–5.90 MG mg/mL at 293, 303, and 313 K) and thermodynamics (calculated activation energy (E_a) = 2.09 kJ/mol) as well as tests of the feasibility of column flushing were conducted using talc to remove MG from aqueous solutions (100% removal after 140 pore volumes of a 12-h run). We studied specific removal behaviors of MG by talc for pH values > 8.0, where MG molecules that had adsorbed onto the talc predominantly changed to the carbinol base form and were retained on the talc.

Keywords: Talc; Malachite green; Kinetic; Thermodynamic; Column flushing

---

1. Introduction

Soluble cationic dyes such as malachite green (MG) used in industrial dyeing and finishing processes cause certain hazardous and environmental problems [1–4]. In the water body into which they are discharged, the presence of these dyes causes undesirable consequences, including unpleasant esthetic effects of the dye wastewater and reduction inthe photosynthetic action of the water flora [5]. Use

---

*Corresponding author.

of MG dye in many industrial applications has adverse effects such as carcinogenesis, mutagenesis, teratogenesis, cytotoxicity, and reduced fertility in humans as well as in fish in aquaculture. The carcinogenic properties of MG, which is used in aquaculture as a fungicide, ectoparasiticide, and an antiseptic [6], are related to the nitrogen group of the molecule (Fig. 1) [1]. Although MG is banned in many countries for use in aquaculture, it is still used illegally because of its low cost and high efficacy [4].

The biological and chemical methods commonly used to remove MG dye from wastewater are not effective. Chemical treatment is costly and complicated, and it produces toxic by-products [3,7].

Several adsorption processes have been investigated as viable alternative technologies for treating dye effluents, including the use of the following: (i) activated carbon-based materials, (ii) biosorbents, and (iii) inorganic materials. These alternatives are attractive because of their simple design, ease of operation, and relatively high efficiency [5]. Research on activated carbon-based materials [8–10] has led to the testing of other low-cost adsorbents. Recently, various biosorbents, including chitosan [11], hyacinth roots [12], sawdust [13,14], oil palm trunk fiber [15], rice straw [16,17], orange peel [18], hen feathers [19], algae [20], fungus [21], dead leaves of the plane tree [22], cellulose [23], wood [24], waste materials [25–29], degreased coffee beans [5], ginger waste [6], and other materials have been studied. These biosorbents are often discarded or burned, which is potentially less expensive, and are usually available in large amounts. In contrast, inorganic materials, a glossary of MG removal by inorganic materials is given in Table 1, including silica/alumina [30], bentonite [31,32], montmorillonite/sepiolite for adsorption of methyl green [33], AMP clay [34], silica gel [35], zeolite [36], magnetic particles [37], ash [38,39], iron humate [40], and talc [41], all have large surface areas and mechanical stability and have also been used to remove MG from aqueous solutions.

However, most studies of this subject to date have not reported on changes in the structure of MG as a member of the triphenylmethane dye family with a behavior of pH-dependent transformation, which is altered by changes in microenvironmental conditions such as the pH, the presence of ions (buffer concentration), and the type of solvent media [35,41–43]. The chemical structure of MG varies according to the solution pH. As shown in Fig. 1, chromatic MG^+ (Fig. 1(b), λ_{max} = 618 nm $\lambda_{max} = 618\,nm$) has a positive and an increased solubility in the pH range from 3.5 to 5.0, but it changes to a carbinol base (Fig. 1(c)) at >pH 8.0. Under highly acidic conditions (pH < 2.0), MG is protonated to MGH^{2+} (Fig. 1(a), λ_{max} = 255 nm). The deep green color exhibited in the pH range from 3.5 to 5.0 changes to cyan at pH values < 2.0, and at pH values > 8.0, MG is colorless. Because inorganic clays spontaneously increase the pH to the range of 9.0–10.0 in aqueous solution, the effects of alkaline conditioning on MG removal by inorganic clays could be important. In addition, Samiey and Toosi [42,43] recently investigated MG alkaline fading and successfully applied silica gel to the MG removal process at pH < 7.0 [35].

Recently, we demonstrated MG removal by talc [41], which is considered a form of MG alkaline

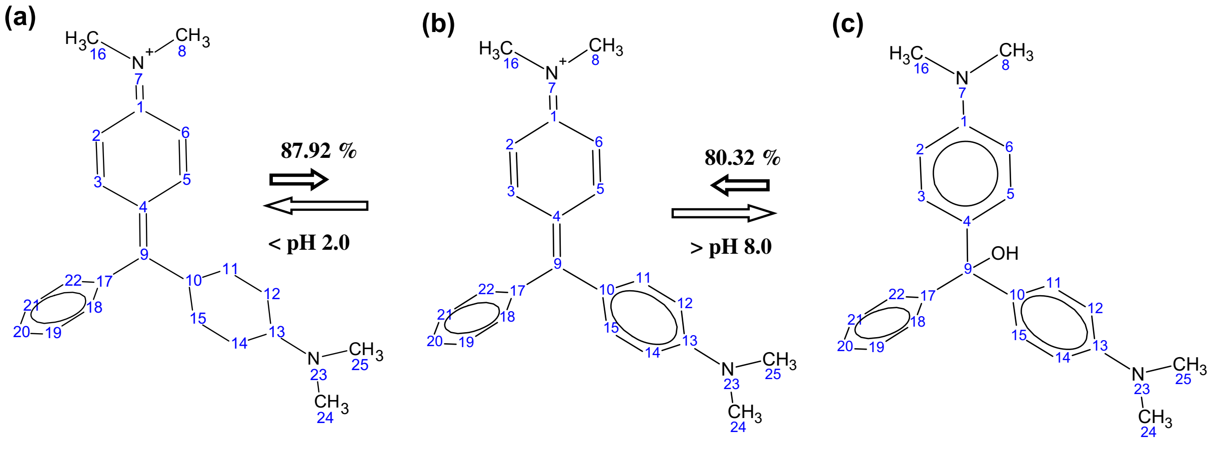

MGH^{2+} Chromatic MG^+ Carbinol base

Fig. 1. Chemical structures of (a) MGH^{2+}, (b) chromatic MG^+, and (c) carbinol base.

Table 1
Elemental analysis (%) of talc observed by X-ray (XRF) spectrometer in this study

MgO	SiO_2	Al_2O_3	Fe_2O_3	CaO	H_2O	Ignition loss
31.84	60.02	1.90	0.13	0.22	0.08	5.81

fading. To measure the MG concentration, an acetate buffer (pH 4.6) was used, with an absorbance calculated at 618 nm of MG showing that a maximum absorbance was used, meaning that the soluble carbinol base should not be considered as a removal percentage because it was not removed by talc. Talc is the most common silicate material, with an ideal chemical formula of $Mg_3Si_4O_{10}(OH)_2$ [44,45]. Its use in the MG removal from aqueous solutions has been reported beyond adsorption isotherms. The specific goals of this study were the following: (i) to evaluate the adsorption kinetics and thermodynamics for three initial MG concentrations (5, 10, and 20 mg/L) and temperatures (293, 303, and 313 K) and (ii) to investigate the feasibility of MG solution flushing by packing talc in the flushing column. The results of this study appear to be useful in the development of processes for MG treatment with inorganic clays.

2. Materials and methods

2.1. Talc and chemicals

All chemicals used in this study were used as received. The cationic dye, MG oxalate (Color Index: Basic Green 4, Classification Number: 42,000, chemical formula = $C_{52}H_{54}N_4O_{12}$, M.W. = 927.00, λ_{max} = 618 nm), was supplied by Sigma-Aldrich (USA). The talc (SP-3000 product; average particle diameter = 2.5 µm; measured Brunauer, Emmett, and Teller surface area = 13.92 m^2/g; density = 0.32 g/cm^3, supplied by Dawon Chemical, Seoul, Korea) composition was characterized according to the manufacturer as shown in Table 1. HCl and NaOH standard solutions (1.0 and 0.1 M) were purchased from DAE JUNG Chemicals (Shiheung, Korea) to adjust the pH of the samples. An acetate buffer solution (pH 4.6) was purchased from Fluka (USA). Double-distilled deionized water (DI water) with a resistance > 18 mΩ was used in all experiments. The stock MG solution (1,000 mg/L) was prepared by dissolving MG in DI water. The experimental solutions were achieved by diluting the MG dye stock solution with DI water in accurate proportions to obtain various initial concentrations [6].

2.2. Measurement of MG concentrations with consideration of MG structural change [41]

To calculate the exact amount of MG, the acetate buffer was used to adjust the pH of the MG solution. The acetate buffer (pH 4.6) caused MGH^{2+} and carbinol base to form MG^+, with equilibrium reached after 2 h. Each sample (3 mL) was then placed into the acetate buffer solution (pH 4.6, 3 mL) for spectrophotometric measurements at a wavelength of 618 nm. The results were used to calculate MG recovery (%) using the following equation.

$$\begin{aligned}\text{MG recovery } (\%) = {} & [\text{abs. intensity of sample at } 618\,\text{nm in acetate buffer (pH } 4.6) \\ & \times \text{ dilution factor}]/[\text{abs. intensity of fresh MG solution } (5\,\text{mg/L}) \text{ at } 618\,\text{nm}]\end{aligned} \quad (1)$$

MG recovery is considered the amount of chromatic MG^+ produced from MGH^{2+} and carbinol base by changing the pH to 4.6. This study was focused on pH > 8.0 because of the basic property of talc in aqueous solution. For MG alkaline fading in basic conditions, the precipitated carbinol base (considered as the removal fraction) and suspended carbinol base (not considered as a removal fraction) were separated to calculate the MG removal efficiency.

2.3. Kinetic and thermodynamic studies

The adsorption kinetics of MG removal by talc was investigated using batch tests. MG solutions (5, 10, and 20 mg/L, 40 mL) were mixed with 0.01 g of talc in 100 mL-brown bottles. To maintain the reaction temperature, the conical tubes were kept in a water bath with constant agitation (293, 303, and 313 K). At appropriate time intervals, samples were collected from the supernatants after centrifugation, and each sample (1 mL) was then placed in the acetate buffer solution (pH 4.6, 1 mL). After 2 h, they were analyzed at 618 nm using a UV–vis spectrophotometer (Scinco, S-3100, Korea). All of the tests were conducted in triplicate to obtain averages of the measurements. Negative control tests without talc were conducted simultaneously to ensure that the adsorption was by talc and not by the containers [17].

2.4. Column experiment [46]

Column flushing experiments were performed with 15 mm × 140 mm columns (Kontes, USA) containing 0.00, 0.10, or 0.20 g of talc mixed well with sand (20–30 mesh, Jumunjin, Korea), corresponding to a bulk volume (10 mL) measured using a 100-mL calibrated cylinder. After packing the mechanically mixed talc and sand into the column, fine sand (2 mL bulk volume) was distributed evenly at the top of column to inhibit talc leakage. The pore volume of the sand in the column was 6 mL. Initially, 10 pore volumes of DI water were pushed through the column with the pack of talc mixed with sand in an upward direction at a flow rate of 1 mL/min, to wet the mixture and avoid floatation of the talc and to saturate inside the column. Then, the MG solution (50 mg/L) was pumped in an upward direction through the column at a flow rate of 1 mL/min. At 6-min intervals, samples were taken and measured at an absorbance intensity of 618 nm. In case of 0.2 g of talc with sand, the test was interrupted after 12 h and then continued again to observe the talc's MG removal characteristics in detail. During the column tests, the flow rate was controlled by a digital pump (Masterflex® L/S®, Cole-Parmer Instrument, USA).

3. Results and discussion

3.1. Preliminary information for measurement of MG concentrations

The absorbance values of MG^+ cations could be assigned three distinct peaks at 317, 427, and 618 nm. As the pH increased beyond 6, these three peaks disappeared, and another peak formed at 255 nm. This last peak was induced by alkali fading of a colorless solution from which 46.9% of the MG was precipitated as a white powder at the end of drying. The remaining 50.6% was considered to be a soluble carbinol base (Fig. 1) [41]. The break of the conjugated double-bonds in the center of the MG^+ molecules reduces the spread of the π orbital, implying a decrease in the delocalization of the electron. Thus, this causes the disappearance of the band at 618 nm with a considerable decrease in the other bands in the visible part of the spectrum [43]. After all, we corrected the MG concentration after determining the MG recovery ratio for the removal experiment. The MG recovery ratio was determined to be 80.32% under alkaline conditions.

3.2. Adsorption kinetics

To select the optimum operating conditions for the full-scale batch process, kinetics information was needed [22]. MG removal by talc was investigated for the initial MG concentrations (5, 10, and 20 mg/L) and temperatures (293, 303, and 313 K) (Fig. 2). The selected amount of talc (0.01 g) was associated with the maximum removal capacity observed in the low talc loading range. As the temperature rose, the time required to reach equilibrium decreased. This was notable at the 20 mg/L initial MG concentration: the time required to reach equilibrium decreased from 720 to 540 to 60 min for temperatures of 293, 303, and 313 K, respectively. In all cases, most of the MG was adsorbed onto talc rapidly within 10 min. The remainder was slowly removed as carbinol base by precipitation. This may be due to the mass transfer between the MG molecules and talc sheets associated with an increased surface activity and kinetic energy of the solute molecules [47]. Interestingly, as the temperature increased at an initial MG concentration of 20 mg/L, the final MG concentration reached at equilibrium increased from 1.17 to 2.94 to 5.90 mg/L. This is related to carbinol base molecules being dispersed to greater degrees at higher temperatures.

The sorption data, characterized by Lagergren pseudo-first-order kinetics, are based on the followed equation [48]:

$$\frac{d_q}{d_t} = k_1(q_e - q) \tag{2}$$

Integration of the above equation with conditions (q values) from t = 0 to t = t results in the following kinetic rate expression:

$$\log(q_e - q_t) = log_{q_e} - \frac{k_1}{2.303} \times t \tag{3}$$

where k_1 is the pseudo-first-order rate constant (min^{-1}) and q_e and q_t are the amounts of MG adsorbed (mg/g) at equilibrium and at time t (min), respectively.

Ho's pseudo-second-order model can be expressed as [49,50] follows:

$$\frac{t}{q_t} = \frac{1}{k_2 q_e^2} + \frac{t}{q_e} \tag{4}$$

where k_2 (g/mg min) is the rate constant of the pseudo-second-order kinetic plot. Fig. 3 shows the kinetic plots for the pseudo-first-order and

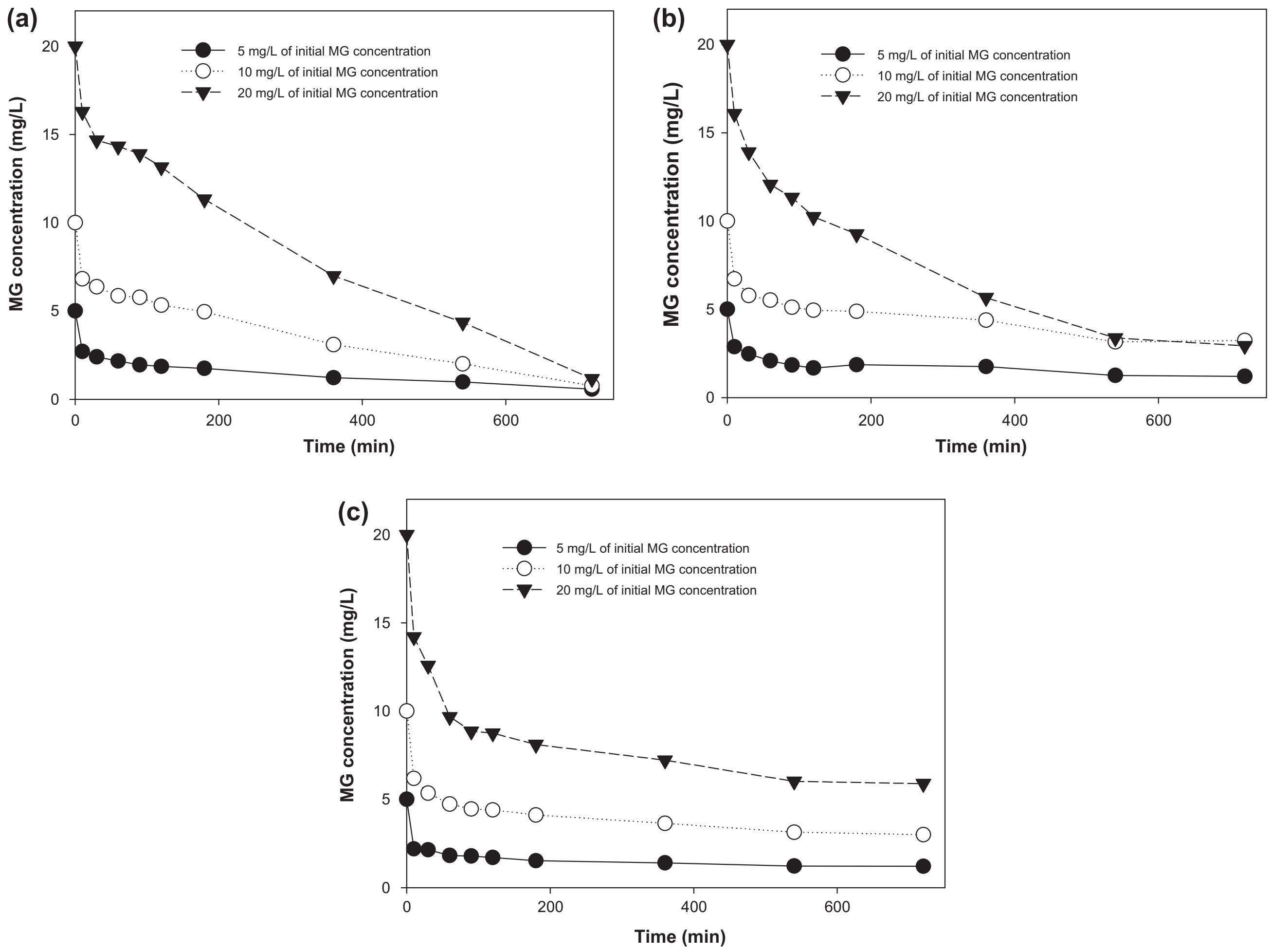

Fig. 2. Adsorption kinetics of MG removal by talc loading (0.01 g/40 mL) at 293 K (a), 303 K (b), and 313 K (c), initial concentration: 5, 10, and 20 mg/L.

pseudo-second-order models as functions of temperature (293, 303, and 313 K). The kinetic constants obtained by linear regression are summarized in Table 2. We could analyze the kinetic constants with pseudo-first-order and pseudo-second-order models. The coefficient of determination (R^2 value) of the pseudo-second-order model is higher than that of the pseudo-first-order model. This indicates that MG adsorption by talc is better fitted with the pseudo-second-order model than with the pseudo-first-order model. It also indicates that the interaction between each solute is stronger than that between MG molecules and talc sheets. These findings agree with previously reported results [6,19].

The Reichenberg equation [51] was applied to determine whether MG adsorption at pH 8.0 obeyed a film- or intraparticle-diffusion mechanism. The equation was analyzed in the following way.

$$B_t = -2.303 \log(1 - F) - 0.4977$$

$$F = Q_t/Q_0 \tag{5}$$

where F is a mathematical function, that is, the fractional attainment of equilibrium at time t, Q_t is the amount of adsorbate uptake at time t, and Q_0 is the maximum equilibrium uptake at an infinite time. By plotting B_t vs. time, the film- and particle-diffusion-controlled mechanism is distinguished [52]: If the graphic line of the plot is a straight line passing through the origin, the adsorption rate is governed by particle diffusion, but if not, it is preferred by film diffusion. The plots of all of the concentrations of MG were nearly linear and did not pass through the origin at 293 K (Fig. 4(a)), indicating that the MG adsorption process was film-diffusion controlled. Fig. 4(b) shows

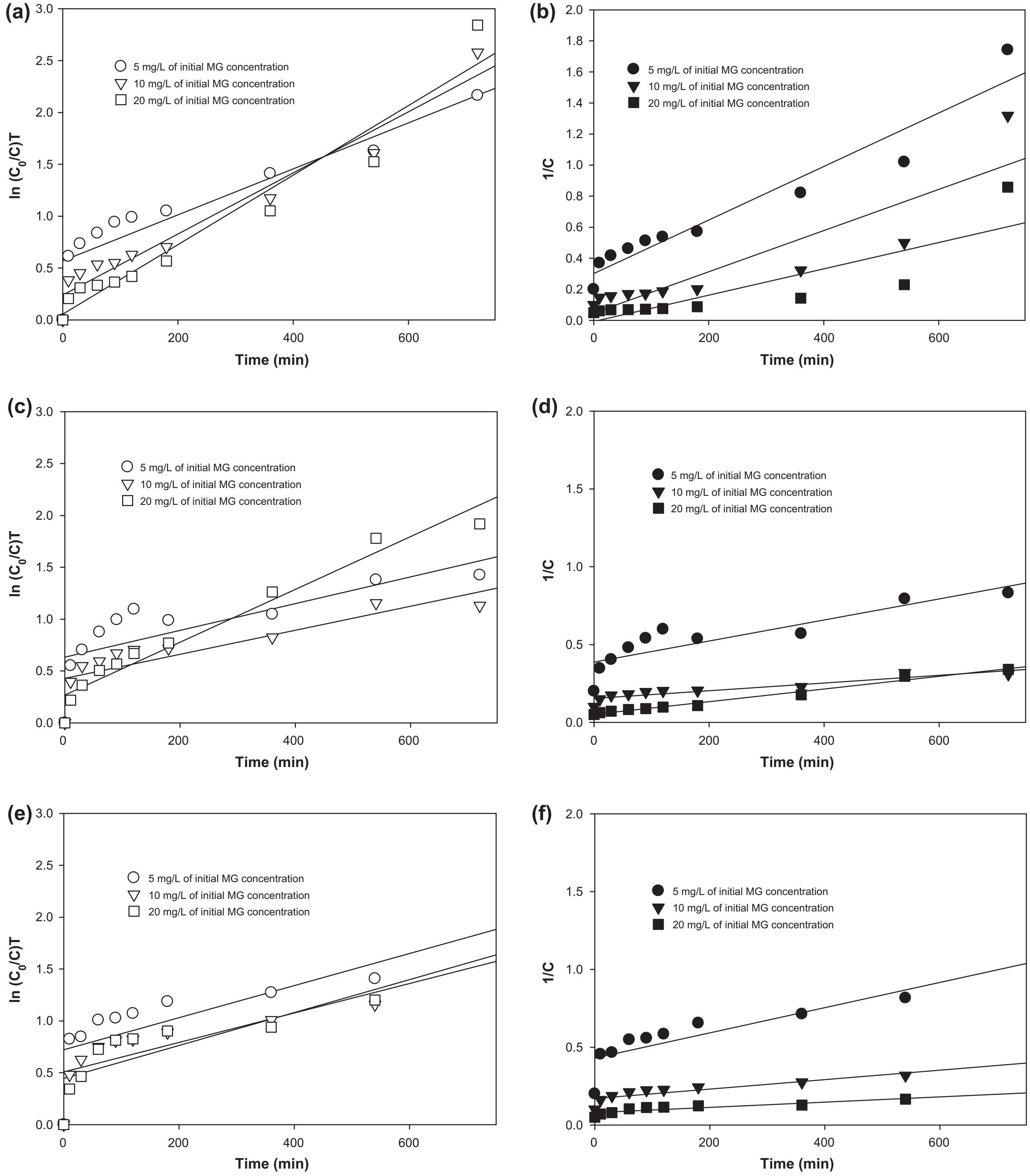

Fig. 3. Thermodynamic study of MG with talc, pseudo-first-order (a, c, and e) and pseudo-second-order (b, d, and f) models for temperature (293, 303, and 313 K), initial MG concentration: 5, 10, and 20 mg/L, talc concentration: 0.01 g/40 mL. Lines do not fit data and used only to guide the eye.

Table 2
Adsorption kinetic parameters for MG (5, 10, and 20 mg/L) with talc (0.01 g/40 mL) according to temperature (293, 303, and 313 K)

		Pseudo-first-order		Pseudo-second-order	
Temperature (K)	Initial MG Concentration (mg/L)	k_1 (min^{-1})	R_1^2	k_2 (g/mg min)	R_2^2
293 K	5	2.22×10^{-3}	0.863	1.72×10^{-3}	0.932
	10	2.95×10^{-3}	0.806	1.33×10^{-3}	0.956
	20	3.35×10^{-3}	0.725	8.48×10^{-4}	0.946
303 K	5	1.29×10^{-3}	0.593	6.78×10^{-4}	0.766
	10	1.16×10^{-3}	0.730	2.49×10^{-4}	0.858
	20	2.55×10^{-3}	0.958	4.07×10^{-4}	0.984
313 K	5	1.55×10^{-3}	0.483	8.11×10^{-4}	0.704
	10	1.42×10^{-3}	0.592	3.04×10^{-4}	0.768
	20	1.59×10^{-3}	0.638	1.68×10^{-4}	0.782

Note: All data were calculated after considering MG recovery, and carbinol base is the soluble portion without precipitation.

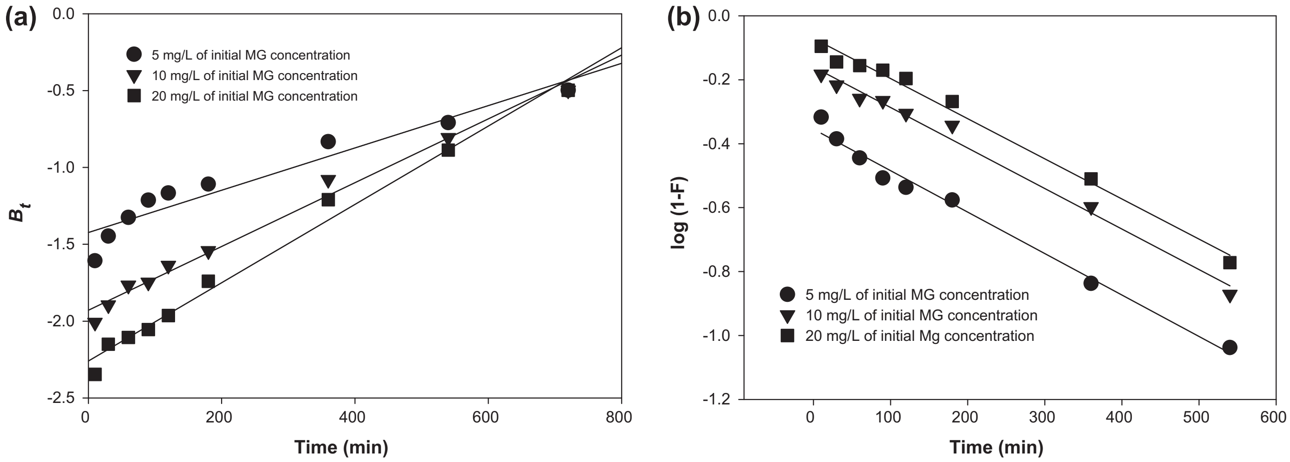

Fig. 4. Plots of B_t vs. time (min) (a) and log $(1-F)$ vs. time (min) for MG adsorption by talc at 293 K, initial MG concentration: 5, 10, and 20 mg/L, talc concentration: 0.01 g/40 mL.

straight lines for log $(1-F)$ vs. time, indicating that MG adsorption onto talc occurs through internal transport, which agrees with reports in the literature [6,19].

3.3. Adsorption thermodynamics

In environmental engineering practice, both energy and entropy parameters need to be considered [22]. To determine whether the reactions will proceed spontaneously or not, Gibb's energy and entropy factors need to be checked. If Gibb's energy change (ΔG^{o}) is negative, the reaction process will occur spontaneously. From information in the literature, we know that the related thermodynamic parameters of the adsorption system are enthalpy change (ΔH^{o}), entropy change (ΔS^{o}), and the equilibrium constant (K). The relationships among these parameters are described by the following equations:

$$\Delta G^{\text{o}} = \Delta H^{\text{o}} - T\Delta S^{\text{o}}$$

$$\Delta G^{\text{o}} = -RT \ln K \tag{6}$$

where K (L/mol) is the equilibrium constant of adsorption, R is the gas constant (8.314 J/mol K), and

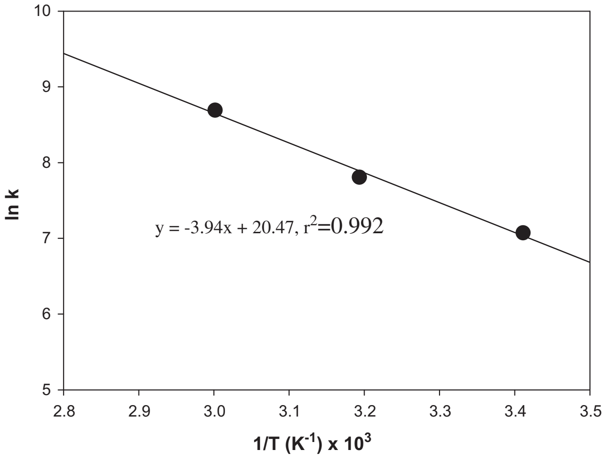

Fig. 5. Arrhenius plot of MG with talc, initial MG concentration: 20 mg/L, talc concentration: 0.01 g/40 mL.

T is the solution temperature in Kelvin (K). The enthalpy (ΔH^{o}) of MG adsorption by talc is determined by the following equation [34,50]:

$$\Delta H^{o} = E_a - RT \tag{7}$$

The activation energy (E_a) for MG adsorption by talc is calculated from the Arrhenius equation.

$$\ln k = \ln A - \frac{E_a}{RT} \tag{8}$$

where A is the Arrhenius frequency factor and k is the rate constant. Fig. 5 displays the Arrhenius equation for an initial MG concentration of 20 mg/L, which was selected because the kinetic results at this concentration were observed to be distinctly different from those at other concentrations. As shown in Table 3, whenever a differential energy change occurs in a system, the ΔH^{o} value is a beneficial parameter to determine whether this reaction is an endothermic or exothermic. A positive value of ΔH^{o} indicates that the interaction of MG is endothermic in nature. Furthermore, positive ΔS^{o} value indicates an increase in the number of degrees of freedom, resulting in MG molecules being randomly adsorbed onto talc sheets. Overall, as the temperature increases, ΔG^{o} decreases, indicating that a higher temperature is energetically favorable. Thus, the reaction will occur spontaneously, which is consistent with reports in the literature [11, 31, 32]. The activation energy (E_a) obtained from the linear Arrhenius equation (Fig. 5), which is $y = -3.94x + 20.47$ ($r^2 = 0.992$), is calculated to be 2.09 kJ/mol. When the value of the activation energy (E_a) is 8–16 kJ/mol, the adsorption process is followed by chemical ion exchange, but when $E_a < 8$ kJ/mol, the adsorption process is physical in nature. When $E_a > 16$ kJ/mol, particle diffusion governs [31,38]. Thus, the adsorption of MG by talc may involve both an activated process and a physical sorption. Physical adsorption, which usually occurs at room temperature, is a faster process than chemical adsorption [10].

3.4. Preliminary column flushing without pH control of the initial MG solution

To study the practical feasibility of MG removal in a continuous mode prior to industrial applications, a column flushing study is essential [53]. Although many efforts in batch modes of MG removal using low-cost materials had been reported, associated column studies have been rarely demonstrated yet. Based on the batch mode results, column tests were conducted for MG removal in a continuous mode [6, 46]. The breakthrough curve points were determined to be at 10, 20, and 45 min for 0.0, 0.1, and 0.2 g of talc load, respectively (Fig. 6). In the presence of talc, the time for the effluent to achieve the initial MG concentration (50 mg/L) by MG flushing was delayed. This can be explained when pH > 8.0 because the removal mechanism is related to adsorption on talc, and an alkaline pH is induced by talc in aqueous media. In case of the talc load of 0.1 g, the final effluent MG concentration was approximately 37 mg/L and remained constant for several hours. In continuous MG solution flushing, the effluent MG concentration approached but did not reach 50 mg/L because of the alkaline fading phenomenon. Thus, the intensity at 618 nm of

Table 3
Thermodynamic parameters for MG with talc (0.01 g/40 mL)

Temperature (K)	E_a (kJ/mol)	ΔH^{o} (kJ/mol)	ΔS^{o} (kJ/mol K)	ΔG^{o} (kJ/mol)
293	2.09	35.192	1.195	−315.245
303		35.276	1.189	−325.206
313		35.359	1.180	−334.424

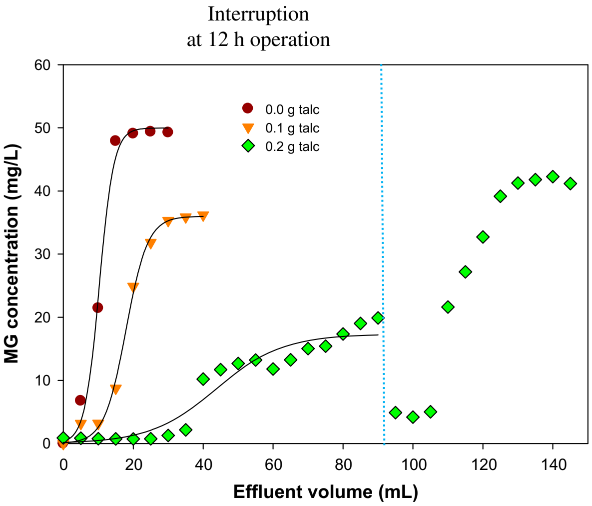

Fig. 6. MG solution flushing of talc packing in the column.

effluent MG solution in acetate buffer (pH 4.6) indicated that nearly 100% was recovered, given the correction of MG recovery efficiency. This finding indicates that the final effluent is not removed by the flushing process in the column. On the other hand, the MG solution reached a concentration of 20 mg/L at 0.2 g talc load after 60 pore volumes of flushing. Only 2 mg of MG were removed before 40 pore volumes of flushing. The final MG recovery efficiency of the effluent observed at 618 nm was 90% by acetate buffer, meaning that approximately 10% precipitated as carbinol base, while the MG recovery efficiency observed at 617 nm was almost 100% after 140 pore volumes of a 12-h run. The removal of MG is dependent on the talc load, although tests at higher talc levels were not successful, due to clogging of clay in the column. The higher adsorption is due to the increase in the surface area of talc, which makes binding sites available for MG removal [54].

3.5. Proposed sorption mechanism

MG was removed by adsorption of a carbinol base onto talc and not by precipitation, as indicated in Fig. 7. In general, pristine talc usually exhibits many stacked plate-like structures (Fig. 7(a)). Because MG is composed of precipitated and soluble carbinol base at pH values > 8.0 [41], after MG adsorption onto talc sheet surfaces, the morphology of the talc becomes more blurred and tough, which is due to the adsorbed carbinol base molecules (Fig. 7(b)). For the precipitated carbinol base ranging from 10 to 20 μm (Fig. 7(c)), those morphologies were not observed. These findings indicate that the carbinol base and the surface of talc interacted via van der Waals forces, weak hydrogen bonding, and steric effects. Therefore, the adsorption mechanism is suggested. After changing MG^+ to a carbinol base, carbinol base molecules are adsorbed onto the talc surface. As a result, suspended carbinol base molecules are not removed at pH > 8.0. This remains as a topic for additional research. Samiey and Toosi avoided MG removal experiments by silica gel at pH > 8.0 because of the MG alkaline fading phenomenon [35].

In examination of talc regeneration, two washings of MG-contaminated talc (1 g) by ethanol (200 mL) resulted in easy desorption. After drying the talc, the MG removal capacity was almost to the same as that of pristine talc. In addition, Scanning Electron Microscopy (SEM) micrograph results were not noticeably different (data not shown). However, the removal capacity of the talc was slightly decreased by residual MG molecules on the talc, most likely because a small fraction of MG was chemisorbed onto talc.

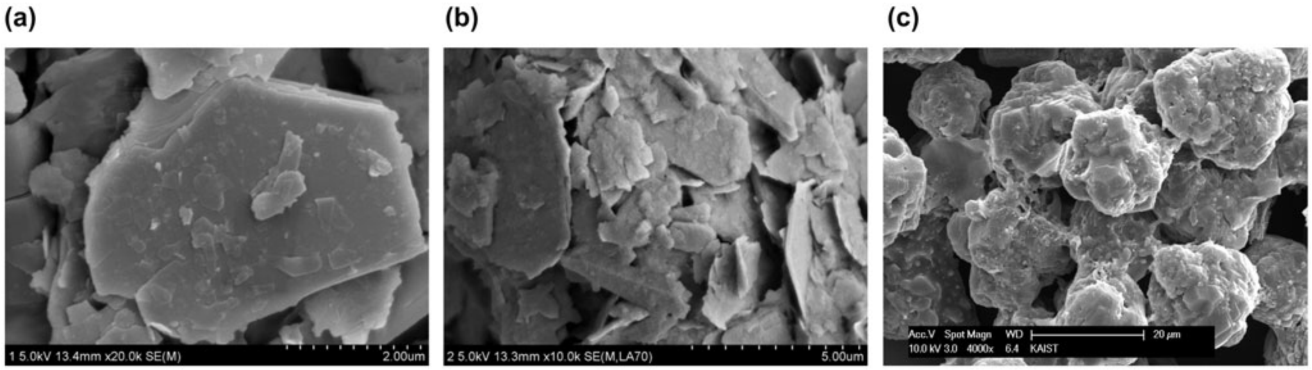

Fig. 7. SEM micrographs of (a) pristine talc, (b) MG adsorbed onto talc at pH > 8.0, and (c) precipitated carbinol base by adjustment with NaOH in the absence of talc.

4. Conclusions

This study demonstrated that adsorption kinetics for MG onto talc followed a pseudo-second-order model. This indicates that the interaction with each solute was stronger than the interaction of MG molecules with talc sheets. Thermodynamically, MG adsorption onto talc was spontaneous and endothermic in nature and increased with the randomness of adsorbed species. Furthermore, tests conducted in continuous column mode demonstrated the feasibility of continuous MG removal by talc. However, MG removal by talc is still challenging at pH > 8.0, which is the case when a soluble carbinol base is produced using inorganic clays. Thus, we are currently studying dynamic adsorption using a larger-scale, fixed bed that is practical for controlling the final pH at <8.0.

Acknowledgment

This work was supported by the Korean Ministry of Environment as a "Converging Technology Project" and the Advanced Biomass R&D Center (ABC) as a Global Frontier Project funded by the Ministry of Education, Science and Technology (ABC-2010-0029728).

References

[1] S.J. Culp, F.A. Beland, Malachite green: A toxicological review, Int. J. Toxicol. 15 (1996) 219–238.

[2] S. Srivastava, R. Sinha, D. Roy, Toxicological effects of malachite green, Aquat. Toxicol. 66 (2004) 319–329.

[3] K. Singh, S. Arora, Removal of synthetic textile dyes from wastewaters: A critical review on present treatment technologies, Crit. Rev. Environ. Sci. Technol. 41 (2011) 807–878.

[4] G. Chen, S. Miao, HPLC determination and MS confirmation of malachite green, gentian violet, and their leuco metabolite residues in channel catfish muscle, J. Agric. Food Chem. 58 (2010) 7109–7114.

[5] M.-H. Baek, C.O. Ijagbemi, S.-J. O, D.-S. Kim, Removal of Malachite Green from aqueous solution using degreased coffee bean, J. Hazard. Mater. 176 (2010) 820–828.

[6] R. Ahmad, R. Kumar, Adsorption studies of hazardous malachite green onto treated ginger waste, J. Environ. Manage. 91 (2010) 1032–1038.

[7] V.K. Gupta, Suhas, Application of low-cost adsorbents for dye removal—A review, J. Environ. Manage. 90 (2009) 2313–2342.

[8] V.K. Gupta, S.K. Srivastava, D. Mohan, Equilibrium uptake, sorption dynamics, process optimization, and column operations for the removal and recovery of malachite green from wastewater using activated carbon and activated slag, Ind. Eng. Chem. Res. 36 (1997) 2207–2218.

[9] K.V. Kumar, Comparative analysis of linear and non-linear method of estimating the sorption isotherm parameters for malachite green onto activated carbon, J. Hazard. Mater. 136 (2006) 197–202.

[10] M.A. Ahmad, R. Alrozi, Removal of malachite green dye from aqueous solution using rambutan peel-based activated carbon: Equilibrium, kinetic and thermodynamic studies, Chem. Eng. J. 171 (2011) 510–516.

[11] Z. Bekçi, C. Özveri, Y. Seki, K. Yurdakoç, Sorption of malachite green on chitosan bead, J. Hazard. Mater. 154 (2008) 254–261.

[12] K.S. Low, C.K. Lee, K.K. Tan, Biosorption of basic dyes by water hyacinth roots, Bioresour. Technol. 52 (1995) 79–83.

[13] S.D. Khattri, M.K. Singh, Removal of malachite green from dye wastewater using neem sawdust by adsorption, J. Hazard. Mater. 167 (2009) 1089–1094.

[14] B.H. Hameed, M.I. El-Khaiary, Malachite green adsorption by rattan sawdust: Isotherm, kinetic and mechanism modeling, J. Hazard. Mater. 159 (2008) 574–579.

[15] B.H. Hameed, M.I. El-Khaiary, Batch removal of malachite green from aqueous solutions by adsorption on oil palm trunk fibre: Equilibrium isotherms and kinetic studies, J. Hazard. Mater. 154 (2008) 237–244.

[16] B.H. Hameed, M.I. El-Khaiary, Kinetics and equilibrium studies of malachite green adsorption on rice straw-derived char, J. Hazard. Mater. 153 (2008) 701–708.

[17] R. Gong, Y. Jin, F.J. Chen, J. Chen, Enhanced malachite green removal from aqueous solution by citric acid modified rice straw, J. Hazard. Mater. 137 (2006) 865–870.

[18] K.V. Kumar, K. Porkodi, Batch adsorbent design for different solution volume/adsorbent mass ratios using the experimental equilibrium data with fixed solution volume/adsorbent mass ratio of malachite green onto orange peel, Dyes Pigment. 74 (2007) 590–594.

[19] A. Mittal, Adsorption kinetics of removal of a toxic dye, malachite green, from wastewater by using hen feathers, J. Hazard. Mater. 133 (2006) 196–202.

[20] K.V. Kumar, S. Sivanesan, V. Ramamurthi, Adsorption of malachite green onto *Pithophora* sp., a fresh water algae: Equilibrium and kinetic modeling, Process Biochem. 40 (2005) 2865–2872.

[21] A.K. Mittal, S.K. Gupta, Biosorption of cationic dyes by dead macro fungus *Fomitopsis carnes*: Batch studies, Wat. Sci. Tech. 34 (1996) 81–87.

[22] O. Hamdaoui, F. Saoudi, M. Chiha, E. Naffrechoux, Sorption of malachite green by a novel sorbent, dead leaves of plane tree: Equilibrium and kinetic modeling, Chem. Eng. J. 143 (2008) 73–84.

[23] C. Pradeep Sekhar, S. Kalidhasan, V. Rajesh, N. Rajesh, Bio-polymer adsorbent for the removal of malachite green from aqueous solution, Chemosphere 77 (2009) 842–847.

[24] H. Zhang, Y. Tang, X. Liu, Z. Ke, X. Su, D. Cai, X. Wang, Y. Liu, Q. Huang, Z. Yu, Improved adsorptive capacity of pine wood decayed by fungi *Poria cocos* for removal of malachite green from aqueous solutions, Desalination 274 (2011) 97–104.

[25] A. Mittal, J. Mittal, A. Malviya, V.K. Gupta, Removal and recovery of Chrysoidine Y from aqueous solutions by waste materials, J. Colloid Interface Sci. 344 (2010) 497–507.

[26] A. Mittal, L. Kurup (Krishnan), Use of waste materials—Bottom Ash and De-Oiled Soya, as potential adsorbents for the removal of Amaranth from aqueous solutions, J. Hazard. Mater. 117 (2005) 171–178.

[27] V.K. Gupta, R. Jain, S. Varshney, Removal of Reactofix golden yellow 3 RFN from aqueous solution using wheat husk—An agricultural waste, J. Hazard. Mater. 142 (2007) 443–448.

[28] A. Mittal, V.K. Gupta, A. Malviya, J. Mittal, Process development for the batch and bulk removal and recovery of a hazardous, water-soluble azo dye (Metanil Yellow) by adsorption over waste materials (bottom ash and de-oiled soya), J. Hazard. Mater. 151 (2008) 821–832.

[29] V.K. Gupta, A. Mittal, A. Malviya, J. Mittal, Adsorption of carmoisine A from wastewater using waste materials—Bottom ash and deoiled soya, J. Colloid Interface Sci. 335 (2009) 24–33.

[30] C. Kannan, T. Sundaram, T. Palvannan, Environmentally stable adsorbent of tetrahedral silica and non-tetrahedral alumina for removal and recovery of malachite green dye from aqueous solution, J. Hazard. Mater. 157 (2008) 137–145.

[31] S.S. Tahir, N. Rauf, Removal of a cationic dye from aqueous solutions by adsorption onto bentonite clay, Chemosphere 63 (2006) 1842–1848.

[32] E. Bulut, M. Özacar, İ.A. Şengil, Adsorption of malachite green onto bentonite: Equilibrium and kinetic studies and process design, Micropor. Mesopor. Mater. 115 (2008) 234–246.

[33] G. Rytwo, S. Nir, M. Crespin, L. Margulies, Adsorption and interactions of methyl green with montmorillonite and sepiolite, J. Colloid Interface Sci. 222 (2000) 12–19.

[34] Y.-C. Lee, E.J. Kim, J.-W. Yang, H.-J. Shin, Removal of malachite green by adsorption and precipitation using aminopropyl functionalized magnesium phyllosilicate, J. Hazard. Mater. 192 (2011) 62–70.

[35] B. Samiey, A.R. Toosi, Adsorption of malachite green on silica gel: Effect of NaCl, pH and 2-propanol, J. Hazard. Mater. 184 (2010) 739–745.

[36] R. Han, Y. Wang, Q. Sun, L. Wang, J. Song, X. He, C. Dou, Malachite green adsorption onto natural zeolite and reuse by microwave irradiation, J. Hazard. Mater. 175 (2010) 1056–1061.

[37] L. Ai, H. Huang, Z. Chen, X. Wei, J. Jiang, Activated carbon/$CoFe_2O_4$ composites: Facile synthesis, magnetic performance and their potential application for the removal of malachite green from water, Chem. Eng. J. 156 (2010) 243–249.

[38] I.D. Mall, V.C. Srivastava, N.K. Agarwal, I.M. Mishra, Adsorptive removal of malachite green dye from aqueous solution by bagasse fly ash and activated carbon-kinetic study and equilibrium isotherm analyses, Colloid Surf. A-Physicochem. Eng. Asp. 264 (2005) 17–28.

[39] V.K. Gupta, A. Mittal, L. Krishnan, V. Gajbe, Adsorption kinetics and column operations for the removal and recovery of malachite green from wastewater using bottom ash, Sep. Purif. Technol. 40 (2004) 87–96.

[40] P. Janoš, Sorption of basic dyes onto iron humate, Environ. Sci. Technol. 37 (2003) 5792–5798.

[41] Y.-C. Lee, J.-Y. Kim, H.-J. Shin, Removal of malachite green (MG) from aqueous solutions by adsorption, precipitation, and alkaline fading using talc, Sep. Sci. Technol. 48 (2013) 1093–1101.

[42] B. Samiey, A.R. Toosi, Kinetics study of malachite green fading in the presence of TX-100, DTAB and SDS, Bull. Korean Chem. Soc. 30 (2009) 2051–2056.

[43] B. Samiey, A.R. Toosi, Kinetics of malachite green fading in alcohol-water binary mixtures, Int. J. Chem. Kinet. 42 (2010) 508–518.

[44] P. Huang, D.W. Fuerstenau, The effect of the adsorption of lead and cadmium ions on the interfacial behavior of quartz and talc, Colloid Surf. A-Physicochem. Eng. Asp. 177 (2001) 147–156.

[45] C. Charnay, S. Lagerge, S. Partyka, Assessment of the surface heterogeneity of talc materials, J. Colloid Interface Sci. 233 (2001) 250–258.

[46] Y.-C. Lee, T.-S. Kwon, J.-S. Yang, J.-W. Yang, Remediation of groundwater contaminated with DNAPLs by biodegradable oil emulsion, J. Hazard. Mater. 140 (2007) 340–345.

[47] O. Martínez-Zapata, J. Méndez-Vivar, P. Bosch, V.H. Lara, Trapping organic molecules in sol-gel aluminosilicate matrices, J. Non-Cryst. Solids 355 (2009) 2496–2502.

[48] S. Lagergren, About the theory of so-called adsorption of soluble substances, Kungliga Svenska Vetenskapsakademiens Handlingar 24 (1898) 1–39.

[49] Y.S. Ho, G. McKay, Sorption of dye from aqueous solution by peat, Chem. Eng. J. 70 (1998) 115–124.

[50] H.-J. Hong, J.-S. Yang, B.-K. Kim, J.-W. Yang, Arsenic removal behavior by Fe-Al binary oxide: Thermodynamic and kinetic study, Sep. Sci. Technol. 46 (2011) 2531–2538.

[51] D. Reichenberg, Properties of ion-exchange resins in relation to their structure. III. Kinetics of exchange, J. Am. Chem. Soc. 75 (1953) 589–597.

[52] R. Ahmad, Sawdust: Cost effective scavenger for the removal of chromium(III) ions from aqueous solutions, Water Air Soil Pollut. 163 (2005) 169–183.

[53] I. Ali, V.K. Gupta, Advance in water treatment by adsorption technology, Nat. Protoc. 1 (2006) 2661–2667.

[54] S.T. Akar, R. Uysal, Untreated clay with high adsorption capacity for effective removal of C.I. Acid Red 88 from aqueous solutions: Batch and dynamic flow mode studies, Chem. Eng. J. 162 (2010) 591–598.